

A formula constituted by arsenic trioxide and dimercaprol enhances sensitivity of pancreatic cancer xenografts to radiotherapy

Jinbin Han (✉ 18621100359@163.com)

Shanghai Jiao Tong University School of Medicine <https://orcid.org/0000-0001-5122-7502>

Ning Wu

Shanghai Pudong New Area Gongli Hospital

Ying Liu

Yunnan Provincial Hospital of Chinese Medicine

Simin Yu

Shanghai Jiao Tong University School of Medicine

Jianmin Zhu (✉ jmzhu@scrc.ac.cn)

Shanghai Clinical Center, Chinese Academy of Science

Research

Keywords: arsenic trioxide, dimercaprol, radiosensitizer, hypoxia, pancreatic cancer stem cells

Posted Date: June 8th, 2020

DOI: <https://doi.org/10.21203/rs.3.rs-33227/v1>

License:  This work is licensed under a Creative Commons Attribution 4.0 International License.

[Read Full License](#)

Abstract

Objective To investigate the efficacy of the formula constituted by arsenic trioxide (ATO) and dimercaprol (BAL), BAL-ATO, as a radiosensitizer against pancreatic cancer xenografts. **Methods** Four treatment arms, including the control, radiotherapy (RT), BAL-ATO and RT + BAL-ATO, were examined using mouse models bearing SW 1990 human pancreatic cancer xenografts. Besides survival and tumor volume analysis, living imaging for cell apoptosis in tumor samples, confocal laser microscope observation for hypoxia, western blot and immunohistochemistry (IHC) assays were employed to detect the mechanism of BAL-ATO in radiotherapy. **Results** The median survival of the combination (RT + BAL-ATO) group (64.5 days) was significantly longer than those of the control (49.5 days), RT (39 days), and BAL-ATO (48 days) groups ($P < 0.001$). Compared to the control group, RT + BAL-ATO inhibited the growth of tumors in mice by 73%, which was much higher than the rate of inhibition of RT alone (59%). The further analysis results also showed an improved microenvironment with regard to hypoxia in tumors treated by BAL-ATO alone or RT + BAL-ATO; besides, the suppression of signals, such as CD24, CD44, ALDH1A1, Gli-1 and Nestin, those associating with pancreatic cancer stem cells (PCSCs), were detected in the tumor samples treated by BAL-ATO alone or RT combining with BAL-ATO. **Conclusion** The data suggested that BAL-ATO, a formula constituted by ATO and BAL, could function as a sensitizer to radiotherapy for pancreatic cancer xenografts, and the mechanism might be attributed to hypoxia reduction and inhibition to signal pathways associated with PCSCs.

Introduction

Pancreatic cancer is ranked as the seventh most common cause of cancer deaths, with 330,000 deaths globally each year [1]. Most pancreatic cancer patients are diagnosed with end-stage disease, and only 10–15% among them have the opportunity for surgery, even though an operation is still the most valid therapeutic method. Patients who lose the opportunity to undergo surgery will inevitably suffer through chemotherapy and/or radiotherapy, and the 5-year survival of pancreatic cancer patients is currently approximately 10% [2].

Radiotherapy is one of the main treatment methods of pancreatic cancer. However, there is an evident difference in the sensitivity of malignant tumors to radiotherapy. Pancreatic cancer is not very sensitive to radiotherapy; even the largest dosage of irradiation that can be tolerated cannot currently produce an ideal clinical response. It is difficult to increase the dose of external radiation alone and achieve satisfactory effectiveness because the pancreas is a retroperitoneal organ and is closely surrounded by normal tissues such as the liver and intestines [3]. The advantage of radiotherapy, either alone or combined with chemotherapy, as a palliative treatment for advanced or relapsed disease is uncertain, and this remedy currently does not demonstrate survival benefits in advanced pancreatic cancer patients [4].

Arsenic trioxide (ATO) is a traditional drug sourced naturally for the treatment of acute promyelocytic leukemia (APL) worldwide, and it is approved for treatment of liver cancer in China [5-7]. We and other investigators have previously reported that ATO has cytotoxic and chemo-sensitizing effects in pancreatic

cancer cells that are at least partially induced by inhibiting the viability of pancreatic cancer stem cells (PCSCs) [8, 9]. However, ATO has demonstrated less efficacy in clinical trials with pancreatic cancer patients, and the dose-related risks of cardiac and hepatic toxicity limit its application clinically [10].

To achieve a response in malignant tumors, several organic arsenics have been designed for anticancer therapy [11]. Their anticancer mechanisms are different from those of ATO, including actions on tumor angiogenesis and metabolism as well as cell signaling pathways [12-14]. A compound called 2,3-dimercaptopropanol, better known as British anti-Lewisite (BAL; dimercaprol) was synthesized by biochemists at Oxford University approximately one century ago and is still stored currently in hospital pharmacies and is occasionally employed in emergencies [15]. The main purpose in producing this compound is managing Lewisite, which is a combination of acetylene and arsenic trichloride, because arsenic ions can be chelated by these molecules to form nontoxic complexes [15].

Both ATO and some ligands with active thiols have been studied as radiosensitizers [16, 17]. ATO has been shown to induce apoptosis in the PCSC subpopulation of pancreatic cancer cells in previous studies *via* inhibition of the Sonic Hedgehog (SHH) pathway [8, 18]. Our study of arsenics showed that the complexes formed by ATO and BAL had similar anticancer effects to ATO and had less toxicity than ATO alone. It was hypothesized that the combination of ATO and BAL could inhibit the viability of PCSCs and improve hypoxia in pancreatic cancer xenografts.

Materials And Methods

Animals, cell culture and reagents

Female athymic nude mice were purchased from Shanghai SLAC Laboratory Animal Co., Ltd. (Shanghai, China) and maintained under specific pathogen-free (SPF) conditions. The human pancreatic cancer cell line used in this study, SW 1900, was obtained from the Cell Bank of the Chinese Academy of Science (Shanghai, China). Both RPMI medium and fetal bovine serum (FBS) were supplied by Gibco Invitrogen (Carlsbad, CA, USA), and cells were maintained in RPMI medium supplemented with 10% FBS. An ATO solution containing 0.9% sodium chloride was provided by Harbin Yida Pharmaceutical Co., Ltd. (Lot.20190102); 2,3-dimercapto-1-propanol was supplied by Tokyo Chemical Industry Co., Ltd. (Lot.WG5MB-AT) and stored in anhydrous alcohol. Other reagents were obtained from Sigma-Aldrich unless otherwise specified. Protocols for animal experiments were approved by the Animal Experimental Ethic Committee of the Ninth People's Hospital, School of Medicine, Shanghai Jiao Tong University.

Preparation of the formula

The combination of dimercaprol and ATO was prepared in water, and the chemical structures formed were detected in an abiotic condition by mass spectrometry. Briefly, the water solution containing ATO and alcohol solution containing BAL were mixed in a tube with a molar ratio of ATO: BAL = 1:6 (an ATO molecule contains double arsenic ions) and stored at 4 °C. Then, a mass spectrometer (UPLC/SFC-MS, Waters, MA, USA) was used to examine the possible chemical structures.

Survival and tumor volume analysis

To establish animal tumor models, sub-confluent hormone-independent SW 1990 cells (5×10^6 per mouse) were injected into 5 mice in one of their flanks. After 3 weeks, mice bearing tumors were sacrificed, and the tumors were harvested. Two of the larger tumors were cut into approximately $2 \text{ mm} \times 2 \text{ mm} \times 2 \text{ mm}$ pieces and then transplanted into mice.

The mice bearing tumors were randomized into the following 4 groups (n = 6): control group: injection of saline containing 1% alcohol (v:v), radiation-treated (RT) group: 1 Gy of total body X-ray radiation along with injection of saline containing 1% alcohol (v:v), BAL-ATO-treated group: injection of freshly prepared BAL-ATO solution, and RT + BAL-ATO group: combined total body RT and BAL-ATO-treatment. The dose of BAL-ATO was indicated by the quality of ATO contained in the prepared mixture. The mice were injected (i.p.) daily with saline or BAL-ATO with a dose equivalent to 30 mg/kg ATO for five days within a week.

An RS 2000 biological system X-ray irradiator (dose rate, 234 cGy/min) was used to irradiate xenografted animals. RT and RT + BAL-ATO groups of mice received 1 Gy of total body irradiation 2-4 hours after injection on Monday, Thursday and Friday followed by a second treatment within a week consisting of only BAL-ATO. The same treatment used in the first week was repeated in the third week.

Survival observation was carried out from the beginning of treatment to time when all of the animals without intervention died. Tumor sizes were measured every 3 days, and volumes (V) were calculated with the following equation: $V = L \times W^2 \times \pi/6$, where L was a tumor length and W was the width. Measurements were performed from the first to the 37th treatment day.

Live imaging, hypoxia analysis and sample collection

Pancreatic cancer xenograft animal models were established using the methods described above, and 6 mice were included in each group. The treatment schedule was the same as the that described above for the tumor growth analysis.

Three mice in each group bearing tumors were imaged using an IVIS Lumina II system (Caliper Life Sciences, Hopkinton MA, USA) equipped with a charge-coupled device camera at 2 days after the last radiation treatment. The mice received i.v. administration of 100 μL of Annexin-vivo 750 (catalog no. NEV11053, PerkinElmer, Inc) and then were anesthetized with 2% isoflurane in 100% O_2 . Images were acquired by recording the bioluminescent signals and were analyzed with Living Image software (Version 4.2, Caliper Life Sciences). After 3 days, the corresponding animals received BAL-ATO treatment 2 hours before HP-RedAPC-MAb (catalog no. HP8-x, Hypoxyprobe, Inc) was administered. The mice were sacrificed on the 26th treatment day. The tumors were then frozen for tissue sections and the frozen tissues sections were subjected to hypoxia analysis by confocal laser scanning microscopy (Leica TCS SP8, Leica Microsystems Inc, Wetzlar, Germany).

The remaining mice (n = 3) in each group were also sacrificed on the 26th day of the treatment, and blood samples for analysis with a blood & gas analysis system (KT-6300, Pioway, Nanjing, China) were drawn from the orbits of the animals before euthanasia. The tumors were harvested and photographed. The removed tumors were separated and then kept for western blot, IHC, TUNEL and H&E staining assays. Besides, the animal organs including brains, livers as well as kidneys were removed for H&E staining.

H&E staining IHC and TUNEL assays

Paraffin-embedded tumor or organic sample slides were dewaxed, rehydrated, pretreated with hydrogen peroxide and washed with PBS. The samples were then stained with hematoxylin and eosin (H&E), followed by rinsing, and the coverslips were mounted onto slides with Permount (Fisher Scientific, San Francisco, CA). For IHC staining, endogenous peroxidase was blocked with 3% hydrogen peroxide, and the tissue samples on slides were then incubated with primary anti-human antibodies, including anti-HIF-1 α (catalog no. ab5168, Abcam), anti-CD24 (catalog no. ab31622, Abcam, Cambridge, UK), and anti-CD44 (catalog no. ab189524, Abcam, Cambridge, UK). Then color visualization was done with SPlink Detection Kits (catalog no. SP-9000, ZSGB-BIO) in accordance with the manufacturer's instruction. TUNEL assay was performed with an *in situ* cell death detection kit (catalog no. 11684817910, Roche Applied Science) referring to the protocol supplied together with the product. All slides were analyzed and photographed by an experienced pathologist.

Western blot analysis

Tumor tissues were washed with cooled PBS, and then samples with sizes of approximately 0.5 cm \times 0.5 cm \times 0.5 cm were placed in EP tubes containing 0.5 ml of lysate solution and kept on ice. The samples were cut into pieces, followed by grinding with an electric grinder and a 30-minute incubation on ice. Protein was extracted with centrifugation and quantified with a BCA protein assay kit (Cell Signaling Technology, Inc. Danvers, MA, USA). Protein samples (30 μ g) were separated with SDS-PAGE and transferred onto PVDF membranes (EMD Millipore, Billerica, MA, USA). The membranes were blocked for 1 hour with 5% non-fat milk solution at room temperature and then incubated with buffers containing primary antibodies, including anti-HIF-1 α (catalog no. ab51608, Abcam), anti-Nestin (catalog no. ab22035, Abcam), anti-Gli1 (catalog no. sc-515781, Santa Cruz Biotechnology), and anti- β -tubulin (catalog no. sc-134237, Santa Cruz Biotechnology, Santa Cruz, CA, USA), overnight at 4 $^{\circ}$ C. Then corresponding Peroxidase-labeled anti-mouse (catalog no. P0217, DAKO) or anti-rabbit (catalog no. P0260, DAKO) IgG secondary antibody were employed to incubate the membranes for 1 hour. The western blot gel image was produced by an Minichemi 610 chemiluminescent imager (Sagecreation, Beijing, China).

Statistics.

Each calculated value representing a result was expressed as the mean \pm standard error of the mean. Differences between groups were analyzed by one-way ANOVA analysis with PRISM software (GrafPad Software, Inc., San Diego, CA, USA). Significant differences between groups were set at $P < 0.05$.

Results

Dimercaprol and ATO formed multiple complexes

The products from the chemical reaction between dimercaprol and ATO were investigated using mass spectrometry. When dimercaprol (BAL) in alcohol was added into ATO in water with a molar ratio of ATO: BAL = 1:6, the solution changed to a cream white color immediately and became clear after mixing for 5 minutes approximately. The MC mass spectrometry results of the solution demonstrated 5 main peaks at 342.89 m/z, 464.88 m/z, 538.79 m/z, 660.77 m/z and 782.44 m/z (An additional figure file showing this, see Additional file 1). These peak values were generated by the chemical structures capturing a sodium ion (plus 23) respectively, indicating that ATO and BAL might form at least 5 structures in solvents (see Additional file 1). After reducing by the atomic weight of sodium, the molecular weights were 318.89, 440.88, 515.80, 637.79 and 759.77, and the formulas were defined as $C_6H_{12}AsO_2S_4$, $C_9H_{18}AsO_3S_6$, $C_9H_{18}As_2O_3S_6$, $C_{12}H_{24}As_2O_4S_8$ and $C_{15}H_{30}As_2O_5S_{10}$. To remain consistent throughout the study, the mixture containing those complexes generated by ATO and BAL using the method described herein was labeled as BAL-ATO, and its dose were labeled by the quantity of ATO contained in.

BAL-ATO enhanced the effect of radiation-induced inhibition of tumor growth

To evaluate the radio sensitizing effect of BAL-ATO *in vivo*, a treatment schedule including 4 arms was administered to 24 mouse models bearing SW 1990 xenografts (Fig. 1A). The noticeable *in vivo* therapeutic effects of BAL-ATO and RT combination treatment were evaluated by survival analysis. The median survival data showed that the RT + BAL-ATO group (64.5 days) lived significantly longer than the control (49.5 days), BAL-ATO (48 days), and RT (39 days) groups ($P < 0.001$, Fig. 1B). There were no significant differences in the survival length between the control and BAL-ATO treatment groups ($P > 0.05$, Fig. 1B).

Changes in the tumor volumes of different treatment groups were pathologically examined within 37 days. At that timepoint, the tumor volume of the RT + BAL-ATO group ($469 \pm 89 \text{ mm}^3$) was significantly smaller than the volume of the RT group, which was subjected only to X-ray radiation ($719 \pm 144 \text{ mm}^3$, $P < 0.01$), the BAL-ATO group ($1636 \pm 193 \text{ mm}^3$, $P < 0.01$), and the control group ($1765 \pm 203 \text{ mm}^3$, $P < 0.01$). Meanwhile, BAL-ATO significantly enhanced the radiation-induced inhibition of tumor growth, with an increase in the tumor doubling time from 17 to 25 days (Fig. 1C, $P < 0.01$) in the animal models. The data also demonstrated that though BAL-ATO could inhibit tumor growth during the treatment, tumor growth was accelerated in the observation time after drug administration.

Molecular apoptosis imaging in live animals is argued for a useful tool to evaluate anticancer treatment currently. To explore the effects of BAL-ATO in radiotherapy in details, each group having 3 mice in the second experiment that underwent the same management schedule described above received live imaging analysis after Annexin-vivo 750 injection on the 22nd day. The luminescence intensity was strongest in the mice of the RT + BAL-ATO group (Fig. 2A). The other 3 mice without received live imaging

in each group were given euthanasia on the 26th day, and tumors harvested (Fig.2B) were subjected to TUNEL and H&E staining assays. In TUNEL assay, more positive cells were detected in RT + BAL-ATO groups than the three others (Fig. 2C, the upper, and see Additional file 2, an additional table file showing this in more detail). Besides, more cell-death characteristics such as cellular shrinkage and nuclear fragmentation were observed in the H&E- stained tissue sections of tumors treated with RT + BAL-ATO (Fig. 2C, the lower). Taken together, these data indicated that the combination of RT + BAL-ATO was dramatically more effective than the single X-ray treatment in inhibiting tumor growth in the mouse models.

BAL-ATO reduced hypoxia in pancreatic cancer xenografts

The mice receiving live imaging were given euthanasia following injection with HP-RedAPC as per the protocol supplied with the kit on the 26th treatment day. After tumor harvesting, the hypoxic conditions of tumors were examined under a laser confocal microscope. Either stronger staining or more positive cells were observed in tumor tissues from mouse models treated with RT, indicating that hypoxia was increased in tumors by X-ray treatment; however, staining of red color was reduced in the BAL-ATO as well as RT + BAL-ATO group, indicating that BAL-ATO treatment improved hypoxic microenvironments in tumors under radiation (Fig. 3A).

Tumor samples harvested from the mice without receiving live imaging on the 26th day were prepared for tissue slides for IHC assay with HIF-1 α antibody, as well as prepared for extracts used in western blot imaging. Downregulation of the HIF-1 α protein was detected in BAL-ATO group and RT + BAL-ATO in either IHC assay (Fig. 3B and see Additional file 1) or western blot (Fig. 3C), being consistent to the trend of hypoxia observed in the frozen tissue slides by the laser confocal microscope.

BAL-ATO Treatment was associated with PCSC signaling pathways

To examine whether BAL-ATO treatment was related to PCSCs, the tumor samples harvested from the 3 mice without receiving live imaging in the second experiment were subjected to biochemical analysis. Expression of the cell surface markers CD44, CD24, and epithelial-specific antigen (ESA) has been discussed to be characteristics of PCSCs frequently [19], and increased expression of CD24 and CD44 could be detected in the RT group by the IHC assay; however, CD24 as well as CD44 expression declined in the BAL-ATO and RT + BAL-ATO groups, indicating that the characteristics of PCSCs was weakened by BAL-ATO treatment alone or together with RT (Fig. 4A and see Additional file 2, an additional table file showing this in more detail). Gli-1, ALDH1A1 and Nestin proteins have been described to be associated with PCSCs [20]. In the western blot assay, downregulation of these proteins was detected in the BAL-ATO and RT + BAL-ATO groups compared to the control (Fig. 4B). Taken together, the results from IHC and WB analysis provided evidence that BAL-ATO could reduce the characteristics of PCSCs, and this function might play an important role to enhance the killing effect of X-ray on pancreatic cancer cells *in vivo*.

BAL-ATO protected the mouse models from radiation injury

Radiation could damage the immune system, lead to bacterial infections and increase the white blood cell (WBC) count, which is a sensitive indicator of infection [21]. In addition to the survival time measured in the first experiment, the protective effects of BAL-ATO administration were investigated in the second animal model experiment. In a routine blood test (RBT), greater numbers of white blood cells were observed in the RT group than in the control group ($P < 0.01$, Table 1); however, the RT + BAL-ATO group showed no significant difference from the control group ($P > 0.05$, Table 1), indicating that BAL-ATO treatment might protect animals from impairment of immunity by X-ray radiation. Besides blood samples, the organs, including the livers, the brain and the kidneys, were removed from mice in each group and subjected to H&E staining. Among the tissue sections stained, the alterations in the liver, such as cell swelling and nuclear disruption, were observed evidently in RT group but were not visible in the three other groups (Fig. 5). Meanwhile, the differences among brains or kidneys were not as obvious as those of the liver (Fig. 5), indicating that the main organ injured by X-ray radiation might be the livers, and BAL-ATO treatment protected this organ from injury.

Table 1 Effects of ATO-BAL on blood of irradiated mice $\times 10^9/L$

	Control	RT	ATO-BAL	RT + BAL-ATO
WBC	16.3 \pm 1.3	29.3 \pm 4.9 **	17.9 \pm 1.2	18.5 \pm 0.8
RBC	7.2 \pm 0.3	7.3 \pm 0.4	6.7 \pm 1.6	7.4 \pm 0.4
PLT	313.3 \pm 18.4	323.0 \pm 42.5	280.0 \pm 24.7	278.7 \pm 10.6
LYM	6.6 \pm 0.4	10.2 \pm 1.7 **	7.1 \pm 0.5	6.3 \pm 0.5

Note: blood samples were collected via withdrawing from the orbits before euthanasia, and then examined immediately (n = 3). **, $P < 0.01$ vs the control.

Discussion

Arsenic trioxide (ATO) is a traditional natural drug used in China to treat some malignant diseases. A few of reports have suggested that ATO could be employed as a radiosensitizer; however, it has a limited threshold of clinical transduction due to its evident toxicity [24-26]. Our group investigated the inhibitory function of ATO in pancreatic cancers, but ATO demonstrated modest inhibition of tumorigenesis in pancreatic cancer xenografts, and it showed dose-related risks of cardiac and hepatic toxicity in clinical trials [8]. To improve the effects of arsenic trioxide on pancreatic cancers, a few clinical drugs that could chelate arsenic cations (As^{3+}) have been examined to determine whether they could form complexes with useful anticancer effects. Among those drugs, dimercaprol (2,3-dimercaptopropanol), also called British anti-Lewisite (BAL) because it was designed as an antidote for lewisite (a now-obsolete arsenic-based chemical warfare agent) by British biochemists during World War II, was found to facilitate ATO in killing pancreatic cancer cells in our study.

A primary CCK-8 test of the cytotoxicity of BAL in pancreatic cell lines was performed before it was used in the animal model experiment, and no significant inhibition was observed when the cells were exposed to cultures containing the compound at concentrations up to 60 μ M (An additional file showing this in more detail, see Additional file 3). During this study, we discovered that the complexes formed by ATO and BAL demonstrated inhibitory capacity similar to ATO *in vitro*, and further study of BAL-ATO demonstrated that the mixture combined with low-dose irradiation could strengthen the capacity to kill pancreatic cancer cells in culture. Therefore, we investigated whether BAL-ATO could function as a radiosensitizer against pancreatic cancer in mouse models.

Before the animal model experiments reported, 5 mice were used to evaluate the system toxicity of the drugs. The animal toxicity experiment demonstrated that BAL-ATO had less system toxicity than ATO or BAL. When it was used at the dose level of 30 mg/kg ATO along with corresponding quantity of BAL, none of the animals could tolerate the monotherapy by either ATO or BAL, but their combination. Therefore, neither ATO nor BAL alone was designed in the normal animal model experiments. Meanwhile, the reported animal experiments indicated that BAL-ATO injection hardly inhibited the tumorigenesis of pancreatic cancer xenografts; however, BAL-ATO combined with low-dose irradiation of X-ray generated evident growth inhibition of pancreatic cancer xenografts. Compared to radiation alone, the combination of X-ray radiation and BAL-ATO prolonged the tumor doubling-time by approximately 2 times, indicating that BAL-ATO might function as a radiosensitizer (Fig. 1C). The mice receiving RT occasionally exhibited diarrhea, weight loss, and mouth ulceration in both the irradiation and the combination groups. Further analysis of blood samples and organs including the brains, the livers, and the kidneys demonstrated that BAL-ATO administration might reduce the injury resulting from X-ray radiation (Fig. 5, and Table 1).

Hypoxia occurs in most solid tumor tissues and is defined as an essential cause of resistance of tumors to radiotherapy [27, 28]. At present, most radiosensitizers consist of compounds containing nitro groups, such as misonidazole and RRx-001 [29-31]. These drugs could result in greater anticancer effects in radiation treatments than radiotherapy alone; however, their toxicity and adverse effects are obvious, which leads to limitation in clinical application. ATO is also being studied as a radiosensitizer [26, 32]. In this study, the formula containing ATO and BAL that could reduce the toxicity of ATO by forming multiple complexes was evaluated whether it was capable of acting as a radiosensitizer *in vivo* also. The results of laser confocal, IHC, and WB analyses showed that BAL-ATO improved hypoxia in the microenvironment of tumor tissues, even for tumors that had undergone irradiation (Fig. 3). Furthermore, our study suggested that hypoxia might be aggravated by irradiation in tumors, and BAL-ATO treatment might have function to alleviate the worsening condition within tumors (Fig. 3).

The existence of human pancreatic cancer stem cells (PCSCs) is supported by increasing evidences, and treatment targeting PCSCs was argued for a strategy to killing cancer cells completely [33]. The subpopulation of PCSCs, defined by expression of the cell surface markers CD44⁺CD24⁺ESA⁺ comprises approximately 0.2-0.8% of all cells in tumor tissues [8, 34]. The sonic hedgehog (SHH) signaling pathway plays a critical role in the survival and proliferation of tissue stem and progenitor cells, and SHH is markedly upregulated in CD24⁺CD44⁺ESA⁺ pancreatic cancer cells compared to CD24⁻CD44⁻ESA⁻ and

bulk cells [35]. Previous studies including ours have proposed that the activity of PCSCs could be reduced by ATO *via* binding to Gli proteins, members of the SHH pathway [8]. In this study, the IHC and the western blot results demonstrated that BAL-ATO treatment downregulated the expression of Gli-1 proteins, meantime, downregulation of ALDH1A1 as well as Nestin proteins, that were indicators of stem cells, were also detected in BAL-ATO-treated tumors by western blot assays (Fig. 4B). Moreover, in the group that was treated with BAL-ATO or BAL-ATO combined with radiation, CD24 and CD44 expression was evidently decreased, indicating that BAL-ATO might suppress the viability of PCSCs (Fig. 4A).

Some compounds, such as disulfiram, have thiol groups, and their metal complexes have been reported to be radiosensitizers against a range of cancers due to their potential to induce oxidative stress [36]. Similar to disulfiram, BAL has thiol groups and has capacity to form multiple complexes with arsenic cations. The data of this study suggested that the BAL-ATO formula constituted by ATO and BAL enhanced the effects of radiation against pancreatic cancer *in vivo*. Furthermore, the mechanism of BAL-ATO in acting as a radiosensitizer was demonstrated to be associated with changes in the hypoxic microenvironment and suppression of PCSC viability. Our study on the structure of BAL-ATO suggested that multiple complexes might be present in the mixture, and a screening test might be necessary to identify the most valuable structure. In summary, due to the tolerable systemic toxicity and significant anticancer effect when combined with radiation, the BAL-ATO formula was proposed to be a radiosensitizer candidate against pancreatic cancer by this study.

Abbreviations

ATO: arsenic trioxide; BAL: British anti-Lewisite; RT: radiotherapy; WB: western blot; IHC: immunohistochemistry; TUNEL: terminal deoxynucleotidyl transferase (TdT)-mediated dUTP nick end labeling; PCSC: pancreatic cancer stem cell; SHH: sonic hedgehog; FBS: fetal bovine serum; H&E: hematoxylin and eosin; ESA: epithelial-specific antigen; RBT: routine blood test; WBC: white blood cell; LYM: lymphocyte; PLT: platelet.

Declarations

Acknowledgements

The authors would like to thank Ms. Na Wang (Fudan University Shanghai Cancer Center) for the experimental assistance in cell culture.

Authors' contributions

Jinbin Han, Jianmin Zhu, and Ning Wu made substantial contributions to the design of the study plan, selection protocol and the design of the methods used in this study. Ying Liu and Simin Yu performed the experiments. Jinbin Han and Ning Wu write this article. All authors contributed significantly to the manuscript, read the manuscript, gave final approval for the version to be published, and take public responsibility for appropriate portions of the content.

Funding

This work was funded by the National Natural Science Foundation of China (81473498); Cross-disciplinary Research Fund of Shanghai Ninth People's Hospital, Shanghai JiaoTong University School of Medicine (JYJC201910). The funders had no role in the study design, data collection and analysis, decision to publish, or preparation of the manuscript.

Availability of data and materials

The datasets generated and/or analyzed during the current study are available from the corresponding authors upon reasonable request.

Ethics approval and consent to participate

Protocols for animal experiments of this study were approved by the Animal Experimental Ethic Committee of the Ninth People's Hospital, School of Medicine, Shanghai Jiao Tong University (HKDL2018329).

Consent for publication

All authors consent to publication.

Competing interests

The authors declare no conflict of interest.

References

1. Rawla, P.; Sunkara, T.; Gaduputi, V., Epidemiology of Pancreatic Cancer: Global Trends, Etiology and Risk Factors. *World journal of oncology* **2019**, 10, (1), 10-27.
2. Huang, L.; Jansen, L.; Balavarca, Y.; Babaei, M.; van der Geest, L.; Lemmens, V.; Van Eycken, L.; De Schutter, H.; Johannesen, T. B.; Primic-Zakelj, M.; Zadnik, V.; Besselink, M. G.; Schrotz-King, P.; Brenner, H., Stratified survival of resected and overall pancreatic cancer patients in Europe and the USA in the early twenty-first century: a large, international population-based study. *BMC medicine* **2018**, 16, (1), 125.
3. Ciabatti, S.; Cammelli, S.; Frakulli, R.; Arcelli, A.; Macchia, G.; Deodato, F.; Cilla, S.; Giaccherini, L.; Buwenge, M.; Morganti, A. G., Radiotherapy of pancreatic cancer in older patients: A systematic review. *Journal of geriatric oncology* **2019**, 10, (4), 534-539.
4. Tian, Q.; Zhang, F.; Wang, Y., Clinical assessment of palliative radiotherapy for pancreatic cancer. *Cancer radiotherapie : journal de la Societe francaise de radiotherapie oncologique* **2018**, 22, (8), 778-783.

5. Yang, H.; Zhou, S.; Shen, R.; Luo, S.; Li, L.; Lin, H.; Chen, H.; Liao, Z.; Lin, W.; Xie, X., Evaluation on Efficacy and Safety of Arsenic Trioxide Plus Transcatheter Arterial Chemoembolization Versus Transcatheter Arterial Chemoembolization alone for Unresectable Primary Liver Cancer. *Asian Pacific journal of cancer prevention : APJCP* **2017**, 18, (10), 2695-2701.
6. Antman, K. H., Introduction: the history of arsenic trioxide in cancer therapy. *The oncologist* **2001**, 6 Suppl 2, 1-2.
7. Beauchamp, E. M.; Uren, A., A new era for an ancient drug: arsenic trioxide and Hedgehog signaling. *Vitamins and hormones* **2012**, 88, 333-54.
8. Han, J. B.; Sang, F.; Chang, J. J.; Hua, Y. Q.; Shi, W. D.; Tang, L. H.; Liu, L. M., Arsenic trioxide inhibits viability of pancreatic cancer stem cells in culture and in a xenograft model via binding to SHH-Gli. *OncoTargets and therapy* **2013**, 6, 1129-38.
9. Chang, K. J.; Yang, M. H.; Zheng, J. C.; Li, B.; Nie, W., Arsenic trioxide inhibits cancer stem-like cells via down-regulation of Gli1 in lung cancer. *American journal of translational research* **2016**, 8, (2), 1133-43.
10. Han, J.; Liu, L.; Yue, X.; Chang, J.; Shi, W.; Hua, Y., A binuclear complex constituted by diethyldithiocarbamate and copper(I) functions as a proteasome activity inhibitor in pancreatic cancer cultures and xenografts. *Toxicology and applied pharmacology* **2013**, 273, (3), 477-83.
11. Rossi, A.; Riccio, A.; Coccia, M.; Trotta, E.; La Frazia, S.; Santoro, M. G., The proteasome inhibitor bortezomib is a potent inducer of zinc finger AN1-type domain 2a gene expression: role of heat shock factor 1 (HSF1)-heat shock factor 2 (HSF2) heterocomplexes. *The Journal of biological chemistry* **2014**, 289, (18), 12705-15.
12. Zhang, Y.; Zhu, X.; Liu, D.; Song, J.; Zhang, H.; Lu, J., Pre-treatment DWI as a predictor of overall survival in locally advanced pancreatic cancer treated with Cyberknife radiotherapy and sequential S-1 therapy. *Cancer imaging : the official publication of the International Cancer Imaging Society* **2018**, 18, (1), 6.
13. Hoffman, E. A.; Gizelska, K.; Mirowski, M.; Mielicki, W., Arsenic trioxide downregulates cancer procoagulant activity in MCF-7 and WM-115 cell lines in vitro. *Contemporary oncology* **2015**, 19, (2), 108-12.
14. Tang, L. R.; Wu, J. X.; Cai, S. L.; Huang, Y. X.; Zhang, X. Q.; Fu, W. K.; Zhuang, Q. Y.; Li, J. L., Prolyl hydroxylase domain 3 influences the radiotherapy efficacy of pancreatic cancer cells by targeting hypoxia-inducible factor-1alpha. *OncoTargets and therapy* **2018**, 11, 8507-8515.
15. Maurel, J.; Sanchez-Cabus, S.; Laquente, B.; Gaba, L.; Visa, L.; Fabregat, J.; Poves, I.; Rosello, S.; Diaz-Beveridge, R.; Martin-Richard, M.; Rodriguez, J.; Sabater, L.; Conill, C.; Cambray, M.; Reig, A.; Ayuso, J. R.; Valls, C.; Ferrandez, A.; Bombi, J. A.; Gines, A.; Garcia-Albeniz, X.; Fernandez-Cruz, L., Outcomes after neoadjuvant treatment with gemcitabine and erlotinib followed by gemcitabine-erlotinib and radiotherapy for resectable pancreatic cancer (GEMCAD 10-03 trial). *Cancer chemotherapy and pharmacology* **2018**, 82, (6), 935-943.

16. Goto, Y.; Nakamura, A.; Ashida, R.; Sakanaka, K.; Itasaka, S.; Shibuya, K.; Matsumoto, S.; Kanai, M.; Isoda, H.; Masui, T.; Kodama, Y.; Takaori, K.; Hiraoka, M.; Mizowaki, T., Clinical evaluation of intensity-modulated radiotherapy for locally advanced pancreatic cancer. *Radiation oncology* **2018**, 13, (1), 118.
17. Koh, H. K.; Seo, S. Y.; Kim, J. H.; Kim, H. J.; Chie, E. K.; Kim, S. K.; Kim, I. H., Disulfiram, a Re-positioned Aldehyde Dehydrogenase Inhibitor, Enhances Radiosensitivity of Human Glioblastoma Cells In Vitro. *Cancer research and treatment : official journal of Korean Cancer Association* **2019**, 51, (2), 696-705.
18. Beauchamp, E. M.; Ringer, L.; Bulut, G.; Sajwan, K. P.; Hall, M. D.; Lee, Y. C.; Peaceman, D.; Ozdemirli, M.; Rodriguez, O.; Macdonald, T. J.; Albanese, C.; Toretzky, J. A.; Uren, A., Arsenic trioxide inhibits human cancer cell growth and tumor development in mice by blocking Hedgehog/GLI pathway. *The Journal of clinical investigation* **2011**, 121, (1), 148-60.
19. Li, C.; Heidt, D. G.; Dalerba, P.; Burant, C. F.; Zhang, L.; Adsay, V.; Wicha, M.; Clarke, M. F.; Simeone, D. M., Identification of pancreatic cancer stem cells. *Cancer research* **2007**, 67, (3), 1030-7.
20. Lee, C. J.; Dosch, J.; Simeone, D. M., Pancreatic cancer stem cells. *Journal of clinical oncology : official journal of the American Society of Clinical Oncology* **2008**, 26, (17), 2806-12.
21. Yazdi, M. H.; Masoudifar, M.; Varastehmoradi, B.; Mohammadi, E.; Kheradmand, E.; Homayouni, S.; Shahverdi, A. R., Effect of Oral Supplementation of Biogenic Selenium Nanoparticles on White Blood Cell Profile of BALB/c Mice and Mice Exposed to X-ray Radiation. *Avicenna journal of medical biotechnology* **2013**, 5, (3), 158-67.
22. Yao, Y. X.; Bing, Z. T.; Huang, L.; Huang, Z. G.; Lai, Y. C., A network approach to quantifying radiotherapy effect on cancer: Radiosensitive gene group centrality. *Journal of theoretical biology* **2019**, 462, 528-536.
23. Li, Y.; Feng, Q.; Jin, J.; Shi, S.; Zhang, Z.; Che, X.; Zhang, J.; Chen, Y.; Wu, X.; Chen, R.; Li, S.; Wang, J.; Li, G.; Li, F.; Dai, M.; Zheng, L.; Wang, C., Experts' consensus on intraoperative radiotherapy for pancreatic cancer. *Cancer letters* **2019**, 449, 1-7.
24. Tomuleasa, C.; Soritau, O.; Kacso, G.; Fischer-Fodor, E.; Cocis, A.; Ioani, H.; Timis, T.; Petrescu, M.; Cernea, D.; Virag, P.; Irimie, A.; Florian, I. S., Arsenic trioxide sensitizes cancer stem cells to chemoradiotherapy. A new approach in the treatment of inoperable glioblastoma multiforme. *Journal of B.U.ON. : official journal of the Balkan Union of Oncology* **2010**, 15, (4), 758-62.
25. Cohen, K. J.; Gibbs, I. C.; Fisher, P. G.; Hayashi, R. J.; Macy, M. E.; Gore, L., A phase I trial of arsenic trioxide chemoradiotherapy for infiltrating astrocytomas of childhood. *Neuro-oncology* **2013**, 15, (6), 783-7.
26. Ning, S.; Knox, S. J., Increased cure rate of glioblastoma using concurrent therapy with radiotherapy and arsenic trioxide. *International journal of radiation oncology, biology, physics* **2004**, 60, (1), 197-203.
27. Petrillo, M.; Patella, F.; Pesapane, F.; Suter, M. B.; Ierardi, A. M.; Angileri, S. A.; Floridi, C.; de Filippo, M.; Carrafiello, G., Hypoxia and tumor angiogenesis in the era of hepatocellular carcinoma transarterial loco-regional treatments. *Future oncology* **2018**, 14, (28), 2957-2967.

28. Patton, M. C.; Zubair, H.; Khan, M. A.; Singh, S.; Singh, A. P., Hypoxia alters the release and size distribution of extracellular vesicles in pancreatic cancer cells to support their adaptive survival. *Journal of cellular biochemistry* **2019**.
29. Droller, M. J., Hypoxic radiosensitizers in radical radiotherapy for patients with bladder carcinoma: hyperbaric oxygen, misonidazole, and accelerated radiotherapy, carbogen and nicotinamide. *The Journal of urology* **2000**, 163, (5), 1600.
30. Meissner, R.; Feketeova, L.; Illenberger, E.; Denifl, S., Reactions in the Radiosensitizer Misonidazole Induced by Low-Energy (0-10 eV) Electrons. *International journal of molecular sciences* **2019**, 20, (14).
31. Oronsky, B.; Scicinski, J.; Ning, S.; Peehl, D.; Oronsky, A.; Cabrales, P.; Bednarski, M.; Knox, S., RRx-001, A novel dinitroazetidone radiosensitizer. *Investigational new drugs* **2016**, 34, (3), 371-7.
32. Ning, S.; Knox, S. J., Optimization of combination therapy of arsenic trioxide and fractionated radiotherapy for malignant glioma. *International journal of radiation oncology, biology, physics* **2006**, 65, (2), 493-8.
33. Chopra, N.; Choudhury, S.; Bhargava, S.; Wajid, S.; Ganguly, N. K., Potentials of "stem cell-therapy" in pancreatic cancer: An update. *Pancreatology : official journal of the International Association of Pancreatology* **2019**.
34. Fitzgerald, T. L.; McCubrey, J. A., Pancreatic cancer stem cells: association with cell surface markers, prognosis, resistance, metastasis and treatment. *Advances in biological regulation* **2014**, 56, 45-50.
35. Bungler, S.; Barow, M.; Thorns, C.; Freitag-Wolf, S.; Danner, S.; Tiede, S.; Pries, R.; Gorg, S.; Bruch, H. P.; Roblick, U. J.; Kruse, C.; Habermann, J. K., Pancreatic carcinoma cell lines reflect frequency and variability of cancer stem cell markers in clinical tissue. *European surgical research. Europaische chirurgische Forschung. Recherches chirurgicales europeennes* **2012**, 49, (2), 88-98.
36. Lee, Y. E.; Choi, S. A.; Kwack, P. A.; Kim, H. J.; Kim, I. H.; Wang, K. C.; Phi, J. H.; Lee, J. Y.; Chong, S.; Park, S. H.; Park, K. D.; Hwang, D. W.; Joo, K. M.; Kim, S. K., Repositioning disulfiram as a radiosensitizer against atypical teratoid/rhabdoid tumor. *Neuro-oncology* **2017**, 19, (8), 1079-1087.

List Of Additional Files

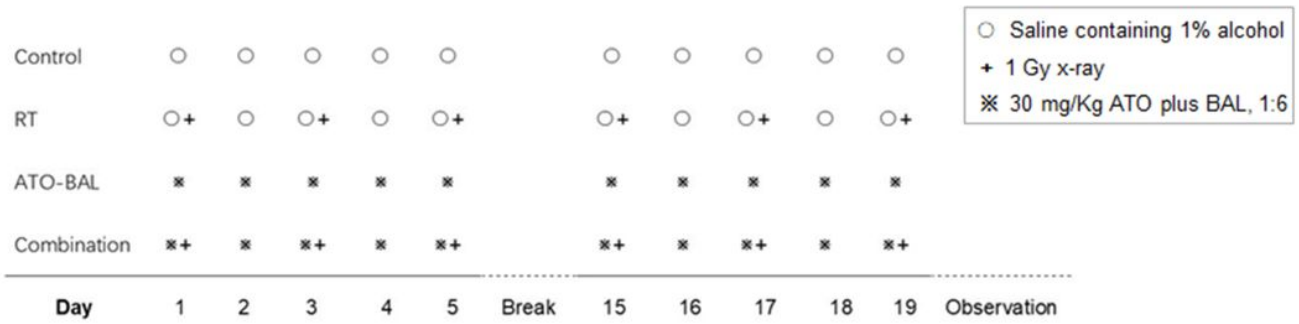
Additional File 1: *PDF, Figure S1*, ATO and BAL formed multiple complexes.

Additional File 2: *PDF, Table S1*, Quantitation of TUNEL, IHC results of tumor samples

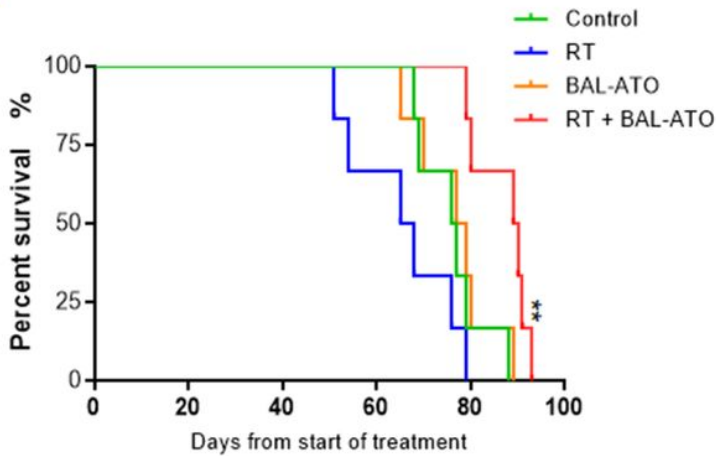
Additional File 3: *PDF, Supplemental Experiment*, In vitro cytotoxicity assay

Figures

A



B



C

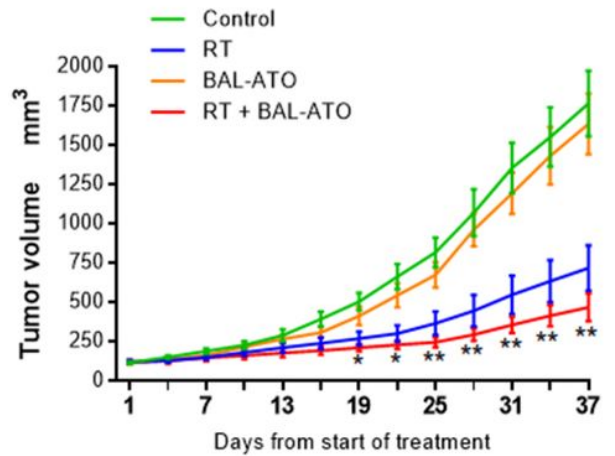


Figure 1

Effect of RT, BAL-ATO and their combination on mice bearing SW 1990 xenografts. (A) Treatment schedule. (B) The median survival time of the groups (days) was analyzed by Kaplan–Meier survival curves and compared using the Log-rank (Mantel-Cox) test. RT + BAL-ATO combination therapy showed a survival benefit compared to the other groups. *, $P < 0.01$ vs the control. (C) Tumor growth chart, indicating the sensitivity of pancreatic cancer to BAL-ATO and radiotherapy. *, $P < 0.05$; **, $P < 0.01$, vs the RT group.

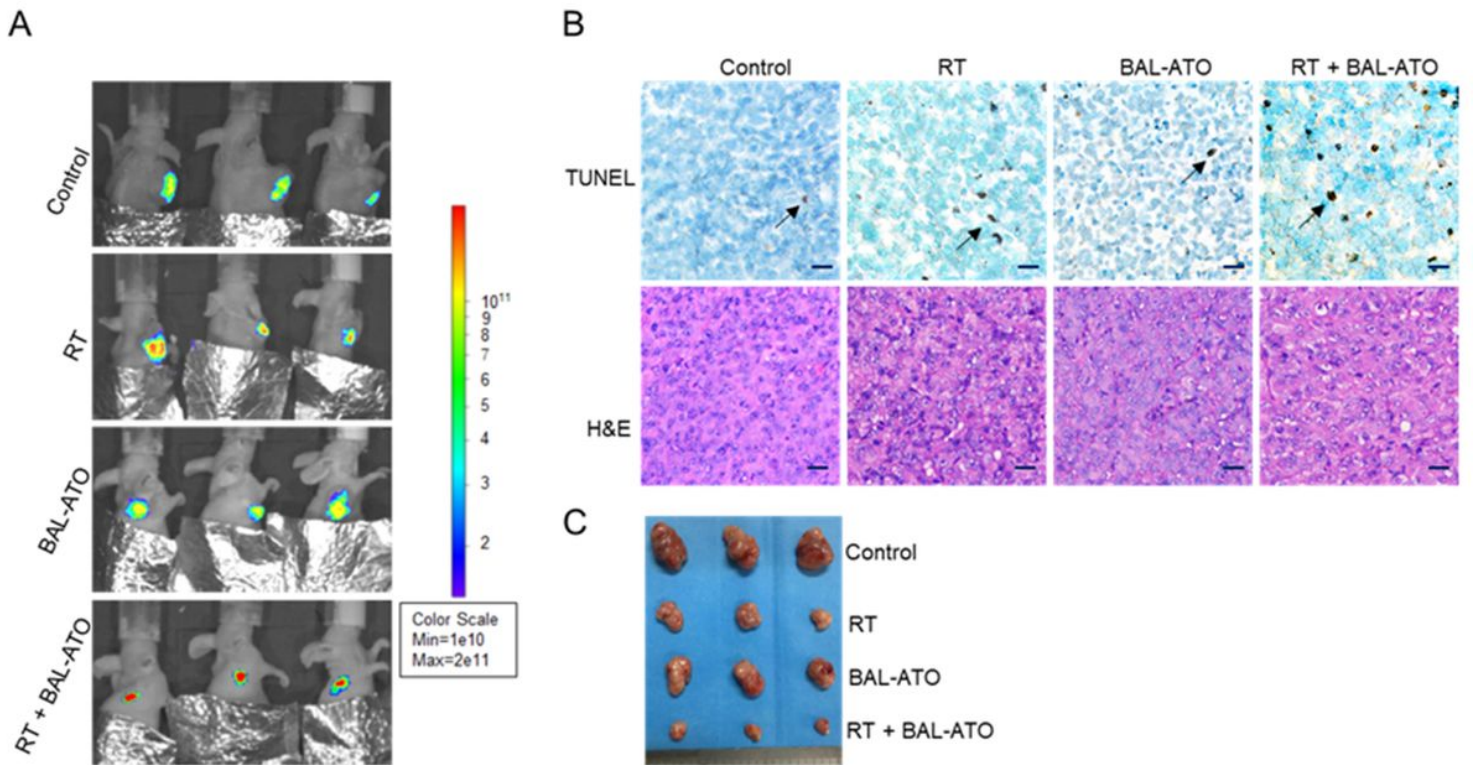


Figure 2

BAL-ATO facilitated X-ray to induce apoptosis in pancreatic cancer xenografts. Mouse models were treated as the schedule shown in Fig. 1A. (A) mice of half number of each group received live imaging after Annexin-vivo 750 injection on the 22nd day ($n = 3$), and RT + BAL-ATO group showed the strongest fluorescence intensity among the groups. (B) Volume comparison by photograph on tumors used in IHC and H&E staining assays. (C) Three mice without receiving live imaging in each group were given euthanasia and tumor samples were harvested on the 26th treatment day ($n = 3$). The upper, more positive-stained cells were detected in the tumors of RT + BAL-ATO group by TUNEL assay (see Additional file 2). The lower, apoptotic cell characters such as nuclear shrinkage or broke were observed in RT + BAL-ATO group by H&E staining. Scale bars, 20 μ m.

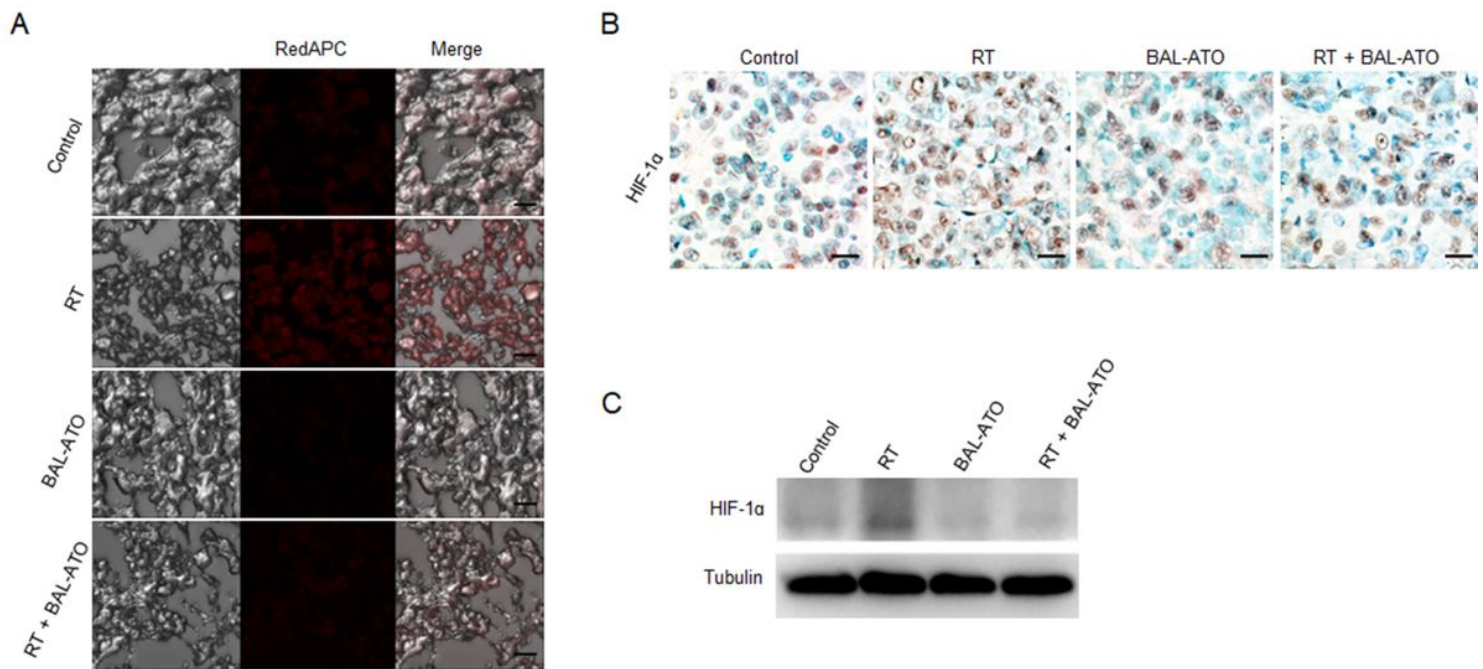


Figure 3

BAL-ATO improved hypoxic microenvironments within pancreatic cancer xenografts. (A) Mouse models the same to ones described in Fig. 2A legend were injected HP-RedAPC-MAb on the 26th treatment day (n = 3). Then the tumors were harvested and prepared for frozen tissue sections used for observation under a confocal laser microscope. Among the tissues, those from tumors treated by RT showed strongest red staining, and those from RT + BAL-ATO group were weak. (B) IHC assay on tumors the same to ones described in Fig. 2B legend (n = 3). A bigger number of and more strongly positive cells were observed in the RT group than in the other groups, and the combination group showed no significant difference from the control group (see Additional file 2). (C) Extracts from tumors the same to ones described in Fig. 2B legend were undergone WB analysis with anti-HIF-1α human antibody, and RT + BAL-ATO group showed a less expression than RT group.

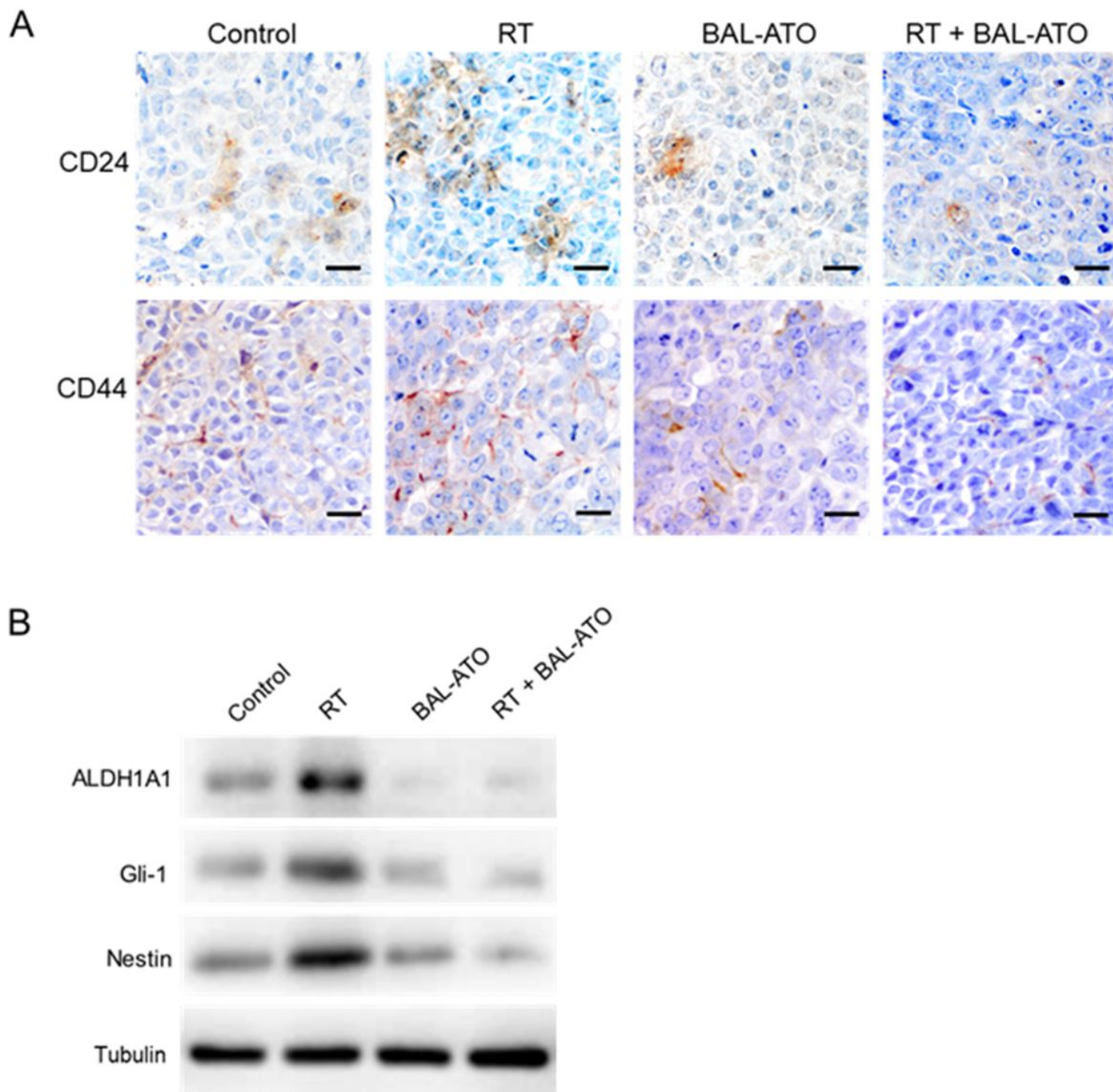


Figure 4

BAL-ATO treatment reduced the PCSC characteristics in pancreatic cancer xenografts. IHC and western blot assays on tumor samples the same to ones described in Fig. 2 B legend (n = 3). (A) Both CD24 and CD44, were evidently decreased in the RT + BAL-ATO group compared to the others. Scale bars, 20 μ m. (B) In the WB assay, the expression of signals associated with PCSCs, including ADLH1A1, Gli-1 and Nestin, were downregulated in either BAL-ATO group or RT + BAL-ATO group.

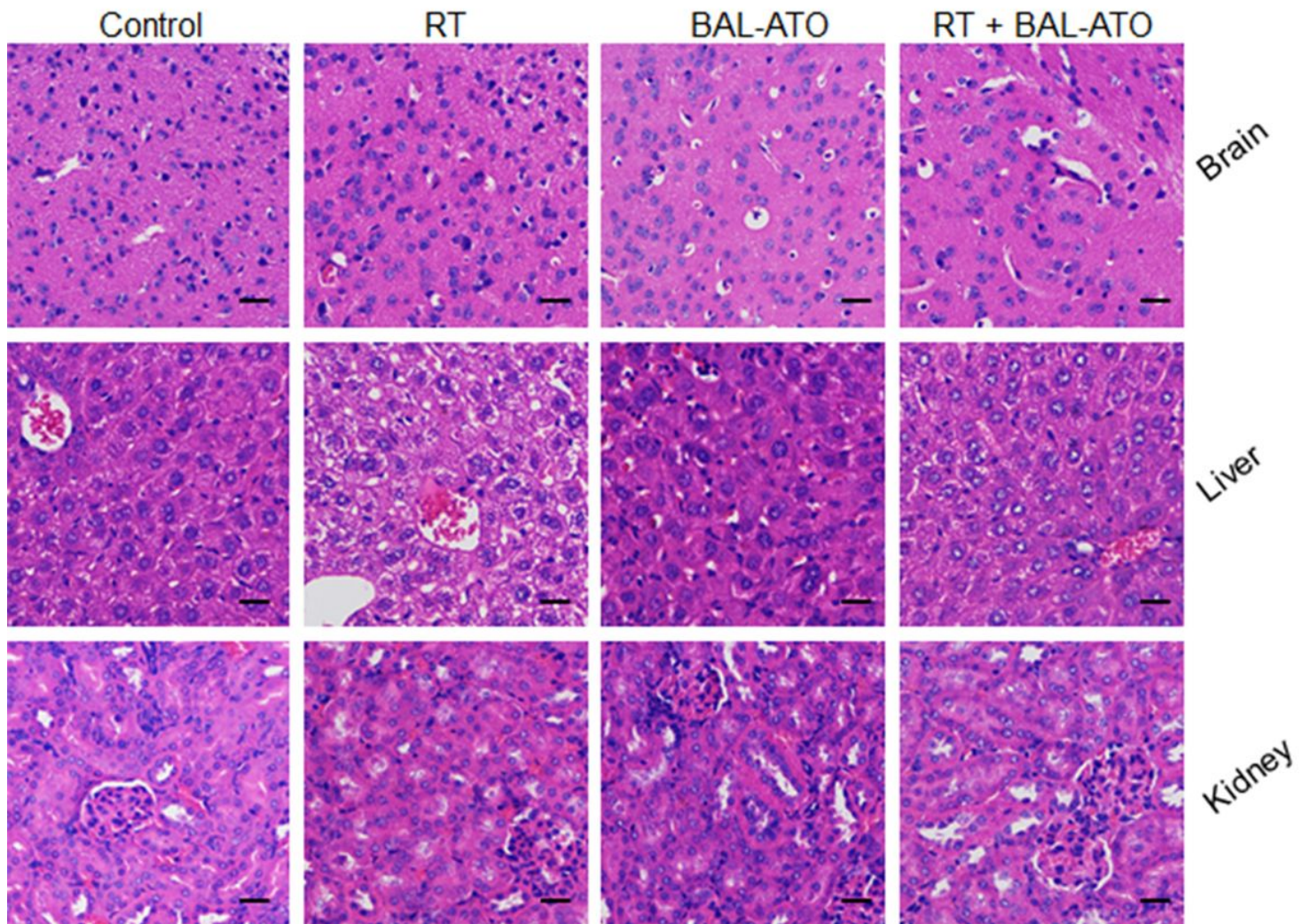


Figure 5

BAL-ATO demonstrated a protective function against X-ray radiation. The organs were obtained from mice the same to ones described in Fig. 2B legend (n = 3). IHC assays were performed on the brains, the livers and the kidneys. Scale bars, 25 μ m.

Supplementary Files

This is a list of supplementary files associated with this preprint. Click to download.

- [supplement9.pdf](#)
- [supplement10.pdf](#)
- [supplement11.pdf](#)